A Virtual Reality Tool for Accuracy Assessment of 3D Models in an Immersive Virtual Environment

Bala Subramaniyam[1], Dharshan Shylesh[2], Jaganathan Ramasamy[2], Navin Kumar[2]

[1]L&T Technology Services, Manapakkam, Chennai – 600 089, Tamil Nadu, India, subramaniyam13@gmail.com
[2]Department of Geography, University of Madras, Guindy Campus, Guindy, Chennai – 600 025, Tamil Nadu, India, dharshansrt@gmail.com, rjnathan@gmail.com, snavinkumar.tvm@gmail.com

Keywords: 3D Textured Models, Unmanned Aerial Vehicles, Accuracy Assessment, Immersive Virtual Reality, Unity Game Engine

Abstract

Accurate validation and assessment techniques are essential for ensuring the reliability of spatial reconstructions derived from photogrammetry, enabling well-informed decision-making across diverse domains. This study presents a Virtual Reality (VR) based accuracy assessment tool tailored for evaluating the accuracy and quality of 3D models generated by Unmanned Aerial Vehicles (UAVs). Leveraging the Unity game engine platform, our workflow entails three key steps: aligning real-world coordinates with an arbitrary Unity coordinate system, transforming the positions of Ground Control Points (GCPs) from field survey to the arbitrary system using a reference GCP, and marking observed points on the 3D models. Absolute and Relative Root Mean Square Errors (RMSE), Mean Errors (ME), and Standard Deviation of errors (SD) are computed within the virtual environment via the game object transform properties. The error distributions around each GCP are visually depicted using Unity game engine components for enhanced interaction and comprehension. The efficacy of the tool is validated through experimentation on four 3D models generated from varying camera angles during UAV data capture. The tool provides the opportunity to directly interact with the 3D models and visualize the errors, which is quite distinct from traditional methods. Using the developed tool, results were obtained to indicate that configurations employing camera angles of 60° + 75º exhibit notable performance in terms of relative and absolute accuracy.

1. Introduction

1.1 UAV 3D Models and Accuracy Assessment

Unmanned Aerial Vehicles (UAV) are an integral component of the Digital Twin era. State-of-the-art computer vision and photogrammetry techniques (Lowe, 2004; Seitz et al., 2006; Furukawa and Ponce, 2007; Snavely et al., 2008; Westoby et al., 2012) are used for dense reconstruction of the 3D world from 2D overlapping images. These dense point clouds are used in the generation of 3D models which have vast applications in the field of natural hazards (Kovanič et al., 2023), cultural heritage site preservation (Pepe et al., 2022), geological mining (Nex and Remondino, 2014), 3D city modelling (Hu and Minner, 2023; Macay Moreia et al., 2013) etc. With a wide range of stakeholders involved, the generation of accurate 3D models is important.

During the process of generating 3D models, a multitude of parameters significantly influence both their spatial accuracy and visual fidelity. While capturing 2D images, a significant role is played by the type of UAV (Room et al., 2019) and mission planning parameters such as mission type, flying height, overlap, and camera angle (Barba et al., 2019; Kang et al., 2019; Manfreda et al., 2019; Rossi et al., 2017). Hybrid data acquisition methodologies are explored, involving the integration of UAVs, Terrestrial Laser Scanners (TLS), and cameras to produce high-quality 3D models (Berrett et al., 2021; Luhmann et al., 2020). An additional critical factor to be carefully addressed during field data acquisition is the configuration, quantity, and quality of Ground Control Points (GCPs), as they wield significant influence on the subsequent reconstruction process, thereby impacting the generation of 3D meshes (D S et al., 2023; James et al., 2017; Liu et al., 2022; Martínez-Carricondo et al., 2018). During the processing stage, a variety of algorithms are employed as feature detectors and descriptors, tasked with extracting keypoints and facilitating their matching (Chen et al., 2021; Singh et al., 2018). All these factors contribute towards the accuracy of reconstruction in the Structure from Motion (SfM) and Multi-View Stereo (MVS) Pipeline. Employing dense point clouds, 3D models are constructed utilizing a variety of techniques, among which prominent methods include Poisson reconstruction and the ball-pivoting algorithm (F. Bernardini et al., 1999; Kazhdan et al., 2006). Naturally, contemporary methodologies are also undergoing experimentation to enhance both the efficacy and the quality of reconstruction.

Given the diverse variables inherent in the generation of 3D models, it becomes imperative to rigorously assess the efficacy and accuracy of each employed technique. While prior studies seen above have predominantly relied on 2D Orthophotos, Digital Surface Models (DSM) and software generated reports to evaluate the accuracy of the 3D reconstruction, they may be insufficient in comprehensively conveying, visualizing, and analyzing errors in a 3D textured model. This is because the conversion of point clouds to 3D models involves data loss through the meshing process which often eliminates fine details and sharp features, thereby compromising accuracy. Notable approaches for error assessment in 3D models include the M3C2 point cloud-to-point cloud distance method (Lague et al., 2013) and point cloud-to-mesh distance analysis. (Moyano et al., 2020) conducted a study to evaluate the quality of 3D models by comparing them with a section profile derived from TLS. These methodologies entail assessing distances between a reference point cloud or profile and a target point cloud or mesh to validate accuracy, which emphasizes more on the relative accuracy side.

1.2 Immersive Virtual Reality and Geospatial Technology

The evolution of the user community has continuously pursued advancements in visualization technologies. A recent innovation gaining prominence is Immersive Virtual Reality (IVR), facilitated by Head Mounted Displays (HMD) that offer deeply engaging experiences. An inherent advantage of this technology is its ability to provide enhanced visualization capabilities.

This contribution has been peer-reviewed. The double-blind peer-review was conducted on the basis of the full paper.
https://doi.org/10.5194/isprs-annals-X-4-2024-333-2024 | © Author(s) 2024. CC BY 4.0 License.

Numerous studies have delved into the fusion of IVR with Geospatial Technology, leveraging its potential for immersive spatial exploration and analysis. (Coltekin et al., 2016) undertook a comprehensive review, focusing on the divisive utilization of 3D visualizations, particularly within immersive geo-virtual environments. This review includes a nuanced discussion of arguments surrounding 3D visualization types, task suitability, and audience preferences. In a study conducted by (Laksono and Aditya, 2019), the Unity 3D Game Engine, along with its Mapbox extension, showcased the development of a web-based viewer integrating OpenStreetMap data and 3D models of real-world buildings within the Universitas Gadjah Mada campus. This study underscores the augmentation of 3D features with building information, attributes, and visual enhancements while highlighting the Unity3D game engine's prowess in providing enhanced user interactions through various viewing modes such as bird’s-eye-view, first-person view, and drone view.

A Virtual Reality (VR) application was developed by (Poux et al., 2020) for creating virtual tours in the Castle of Jehay, Belgium. This work gives a detailed workflow of the application including the 3D model creation process (data capture, processing and rendering), along with a thorough analysis of user requirements. This workflow not only accommodates user convenience but also allows for the creation of new templates, surpassing the limitations of traditional 360º videos. In the context of urban planning, effective community involvement is crucial for informed decision-making and sustainable development. (Szczepańska et al., 2021) proposes leveraging VR technology, exemplified by the ArchitektVR application, to enable immersive and accessible public consultations for planned land development projects, fostering inclusive decision-making despite social distancing constraints. By harnessing VR's capabilities in 3D visualization, this approach empowers stakeholders to comprehend and engage with proposed urban development remotely, fostering inclusive decision-making despite not physically being present.

Within the realm of volcanic research, novel virtual digitization and measurement tools have been developed to facilitate immersive field surveys (Antoniou et al., 2020; Bonali et al., 2024; Gerloni et al., 2018). These tools have been applied across distinct sites: the Metaxa Mine region in Greece, the Dallol volcano in Ethiopia, Santorini in Greece, Mount Etna in Italy and volcanic zones in Iceland. This innovative approach has significantly contributed to volcanic research, education, and outreach initiatives (Tibaldi et al., 2020). Utilizing UAV-based 3D reconstruction, the study sites are carefully surveyed before seamlessly integrating the models into the Unity game engine. Subsequently, a VR application is crafted, featuring specialized tools tailored for diverse spatial operations and seamless navigation within the surveyed sites. These studies on volcanic sites illustrate data quantification and capturing within the virtual environment, making it essential to assess the accuracy of the 3D models used for the survey.

1.3 Problem Statement and Objectives

Through an analysis of studies conducted on 3D models generated from UAV data, a notable observation emerges regarding the scarcity of significant methodologies or visual frameworks for directly assessing the accuracy of these models through intuitive interactions. For example, procedures akin to manually identifying GCPs on orthophotos or Digital Surface Models (DSMs) using a computer screen are notably absent. Existing techniques have emphasized more on the relative distance errors. Conversely, investigations into IVR have showcased a diverse array of possibilities for integrating various aspects of Geospatial Technology. Most of the IVR applications discussed above involves a degree of decision-making and data capture that is highly dependent on the quality of the 3D model geometry. This motivates our exploration into the potential of IVR for conducting operations such as accuracy assessment on 3D models generated from UAV data. Therefore, the objectives of our study encompass the development of a workflow for performing accuracy assessment on 3D models within an immersive virtual environment, along with an evaluation of the advantages associated with such an approach. Subsequently, a validation will be conducted on 3D models generated from multiple UAV camera angles using the developed tool, followed by an in-depth discussion of the obtained results.

2. Methodology

This section describes the workflow employed in the development of the VR accuracy assessment tool. The Unity 3D game engine offers a conducive environment for VR application development, supported by the XR interaction toolkit to establish better user engagement. The tool was developed as a prototype VR application designed to run on a Windows device. The development and study were conducted on a laptop workstation having an AMD Ryzen 7 6800 HS processor, 16 GB of DDR5 RAM and NVIDIA RTX 3060 6GB Graphic card. The Unity editor version used for development is 2021.3.22f1 along with an Oculus Quest 2 HMD. The 3D models derived from UAV data processing are imported as .obj files into the Unity scene. Figure 1 illustrates the sequential progression of functions or operations to be executed. The workflow is categorized into three distinct steps, each elaborated upon subsequently.

2.1 Setting the Reference GCP as the 3D Model Pivot

During UAV surveys, artificial boards or markers with contrasting colors are typically positioned in the study area for the GCP survey. Among them, one GCP, preferably in the central region of the study area, along with its real-world coordinates, serves as the Reference GCP for the study area. Following the initialization of the VR application, the user navigates to the Reference GCP and precisely positions the ray interactor at the center of the GCP marker (see Figure 2). Upon pressing the Trigger button in the VR controllers, a purple sphere is generated at the center of the Reference GCP (see Figure 3) and the 3D model is set as a child object of the newly instantiated sphere, referred to as the Reference sphere. As Unity's hierarchical structure implies, once an object becomes a child of any other object, it inherits the Transform parameters (position, rotation, and scaling) from its parent. Therefore, any modification in the transform parameters of the Reference sphere will consequently adjust the transform parameters of the 3D model. With the Reference sphere positioned over the Reference GCP, the pivot point of the 3D model is now defined by the Reference GCP. In Unity, the pivot point refers to the specific point within an object or 3D model along which the position, rotation and scaling of the object are adjusted. The Reference sphere is repositioned to the origin of the Unity coordinate system (0, 0, 0) effectively placing the 3D model, via the Reference GCP, at the origin of the Unity coordinate system. This enables the Reference GCP real-world coordinates to serve as an offset for incorporating other GCPs. Establishing this reference is essential for accurate subsequent measurements and calculations, thereby ensuring precise error assessment.

This contribution has been peer-reviewed. The double-blind peer-review was conducted on the basis of the full paper.
https://doi.org/10.5194/isprs-annals-X-4-2024-333-2024 | © Author(s) 2024. CC BY 4.0 License.

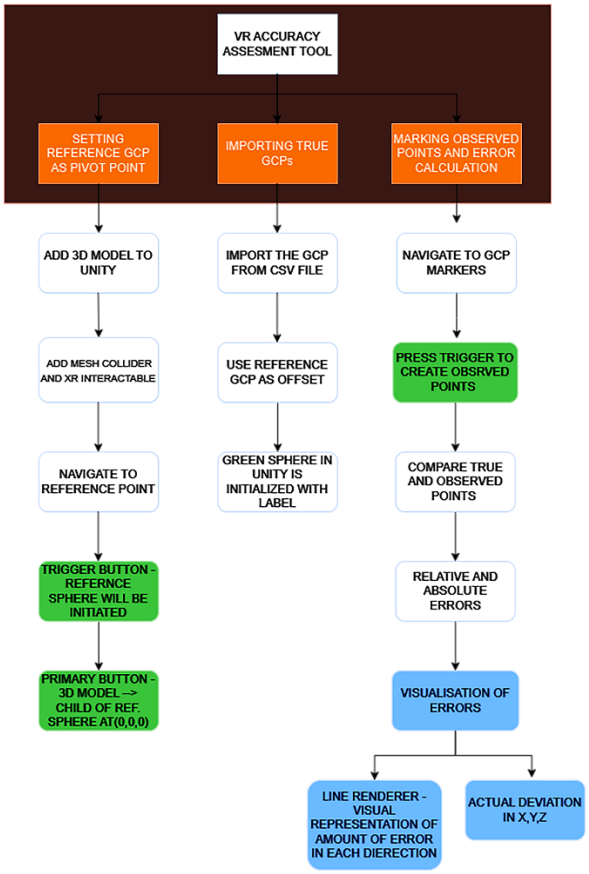

Figure 1. Workflow for the VR tool. The orange boxes represent the three major development steps of the VR tool. The green boxes indicate specific operations using the VR controllers. The blue boxes denote procedures related to error visualization.

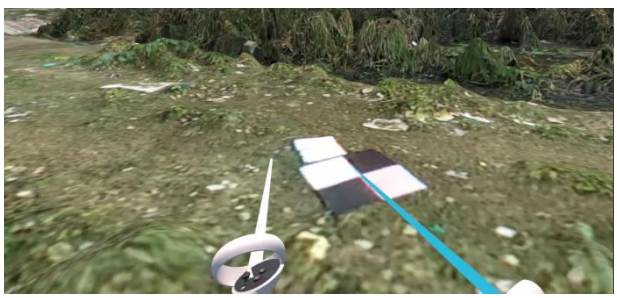

Figure 2. Ray interactor on top of the Reference GCP

Figure 3. Creation of the Reference sphere in the ray interactor position when trigger pressed

2.2 Importing the True GCPs (Checkpoints)

The Reference GCP in the 3D model is now positioned at the origin of the Unity coordinate system. The position of the other GCPs in the Unity coordinate system shall be determined by computing the difference between their real-world coordinates and the Reference GCP real-world coordinates. The GCPs containing the real-world coordinates are imported via a CSV file into the application and on computing the differences their positions in the Unity coordinate system are determined. Sphere game objects are instantiated at the determined Unity coordinates and their color is set to green as shown in Figure 4. These newly instantiated spheres will be referred to as the True spheres or True GCPs, representing the actual real-world position of the GCPs within the study area. Labels for each True GCP are provided to identify their names, which will be used for matching in later stages. They function similarly to Checkpoints. This transformation of real-world data into the virtual space serves as the reference for spatial error analysis and visualization.

2.3 Creation of Observed Points and Calculation of Errors

The user interacts with each GCP marker by navigating around the 3D model. Utilizing the ray interactor, the user points at the centre of a GCP marker to instantiate a sphere referred to as the Observed sphere, depicted in grey color (see Figure 5). A user-friendly interface facilitates the input of names for each Observed sphere, enabling the matching with True spheres identified by labels atop each sphere. This aids in error calculation by comparing Observed and True sphere positions, a process iterated across all GCP markers within the study area. Upon marking all GCPs, an Accuracy Assessment ensues, comprising Absolute and Relative error assessments. The discrepancy between Observed and True sphere positions across all GCPs is quantified using the Root Mean Square Error (RMSE), Mean Error (ME) and Standard Deviation of the errors (SD) statistical techniques, with calculations conducted for x, y, and z coordinates. The RMSE technique has been widely adopted in various studies (Liu et al., 2022; Martínez-Carricondo et al., 2018; Sarkar et al., 2023; Stott et al., 2020) and is used as a benchmark to evaluate the errors. The formula for the Absolute error, Relative error, RMSE, ME and SDE are given below.

$$\text{Absolute error} = \text{Observed value} - \text{True value} \quad (1)$$

$$\text{RMSE} = \sqrt{\frac{\sum_{i=1}^{N}(\text{Observed value}_i - \text{True value}_i)^2}{N}} \quad (2)$$

$$\text{ME} = \frac{\sum_{i=1}^{N}(\text{observed value}_i - \text{True value}_i)}{N} \quad (3)$$

$$\text{SD} = \sqrt{\frac{\sum_{i=1}^{N}(\text{Absolute error}_i - \text{ME})^2}{N}} \quad (4)$$

where N = number of Observed points or spheres

To assess relative accuracy, the disparities in distances between every pair of Observed spheres and True spheres were computed. The number of pairs for assessment is derived by using the combination formula ${}_N C^2$ where N is the number of Observed points. These distance differentials called the Relative error were also subjected to the RMSE, ME and SD analysis to gauge the relative accuracy of the 3D model.

$$\text{Relative Error} = \text{d of Observed pair} - \text{d of True pair} \quad (5)$$

This contribution has been peer-reviewed. The double-blind peer-review was conducted on the basis of the full paper.
https://doi.org/10.5194/isprs-annals-X-4-2024-333-2024 | © Author(s) 2024. CC BY 4.0 License.

where d = distance between the two GCPs in a single pair.

Furthermore, following error calculation, visual representations of errors are created utilizing the Line Renderer component within the Unity platform. Specific colors have been assigned to the error lines to represent errors in each axis: red for the x-axis, blue for the y-axis, and green for the z-axis. By hovering the ray interactor over individual Observed spheres, the degree of deviation from the corresponding True GCP is displayed, facilitating comprehensive error analysis and assessment.

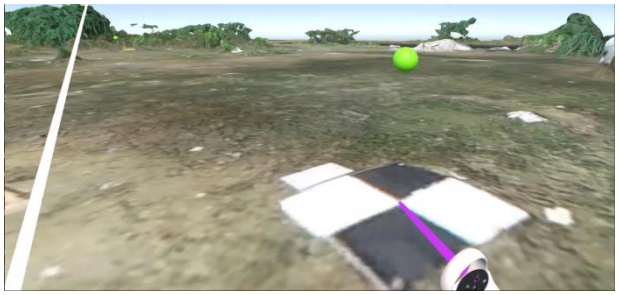

Figure 4. The True sphere (Green color) visualized within the application

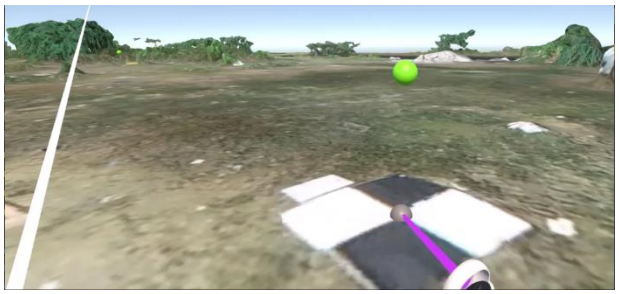

Figure 5. The Observed sphere (Grey color) instantiated on the center of a GCP Marker

3. Experiment

A research experiment was conducted to evaluate the impact of varying camera angles and flight configurations on the absolute and relative accuracy of 3D models, employing the Virtual Reality Tool developed using the above methodology (Section 2). The study was conducted within a small residential area spanning 1.3 hectares located in the northern region of Chennai, India. This area encompasses residential structures, open spaces, road networks, and vegetation, characterized by its predominantly flat terrain. In this experiment, the UAV survey, field survey and data processing parameters were kept constant for the generated 3D models, as discussed below.

3.1 UAV Survey

Three UAV missions were conducted in the region, employing different camera angles of 60°, 75°, and 90°, while maintaining a consistent flying height of 40 meters. The missions utilizing camera angles of 60° and 75° employed a double gridding approach, whereas the mission employing a 90° angle utilized a single gridding approach. Further specifics regarding the UAV flights can be found in Table 1.

Sl. No	Parameters	Description		
1.	Model name	DJI Phantom 4 Pro v 2.0		
2.	Date & Time	26-Nov-2023; 12:15 – 03:00 PM IST		
3,	Flying height	40 [m]		
4.	Flight speed	3.5 [m/s]		
5.	Average GSD	1.15 cm/pixel		
6.	Weather condition	Partly cloudy		
7.	FO / SO	80% / 80%		
8.	Angle of the camera	60º	75º	90º
9.	Mission Type [Grid]	Double	Double	Single
10.	Number of Images	231	231	112

Table 1. UAV Flight Parameters

3.2 GCP Survey

To conduct the accuracy assessment of the 3D models, a total of 21 GCPs were positioned across the study area, with one GCP designated as the Reference GCP. The GCP markers, ranging in size from 35 cm x 35 cm to 70 cm x 70 cm, were evenly distributed horizontally within the study area. The surveying of GCPs was performed using a Sokkia CX-105 survey grade Total Station (TS) whose angular measurement accuracy is 5" and distance measurement accuracy is 3 (+2 ppm x Distance) mm.

3.3 Data Processing

Following the survey, image processing was conducted to produce four distinct 3D models corresponding to varying camera angles: 60°, 75°, a composite of 60° + 75°, and a composite of 75° + 90°. Data processing was performed utilizing the WebODM software from Open Drone Map, with key specifications outlined in Table 2. Georeferencing using the GCPs was not performed for any of the 3D models. A consistent set of parameters was applied throughout the processing. Post the generation of the 3D models, each model underwent validation using the VR Accuracy Assessment tool developed.

Sl. No	Parameter	Description
1.	Software	WebODM
2.	Mesh octree depth	12
3.	Mesh size	10 million triangles
4.	Feature quality	High
5.	Min number of features	15,000
6.	Matcher Type	Bag of Words (bow)
7.	SfM Algorithm	Incremental
8.	Point cloud quality	High
9.	GCPs	Nil

Table 2. Processing options for the generation of 3D models

4. Results and Discussion

4.1 Performance of the Accuracy Assessment Tool

The outcomes derived from the deployment and assessment of the tool illustrate its efficacy in conducting Accuracy Assessment procedures. The tool's functionalities were comprehensively evaluated across multiple dimensions, encompassing locomotion within the scene, usability, visualization, and reliability. Primarily, regarding locomotion within the scene, the tool was intentionally engineered to afford users seamless navigation across all spatial dimensions. Movement velocities were calibrated to a standard rate to mitigate the risk of motion-

induced discomfort. Additionally, the inclusion of Snap Turn functionality allows users to pivot at fixed intervals of 45°, facilitating navigation around GCPs, user interface elements, and other pertinent features. Notably, an important element within the locomotion framework is the integration of 3D teleportation capability, enabling users to swiftly traverse the study area (see Figure 6). This feature circumvents the necessity for continuous locomotion, mitigating the potential for motion-induced discomfort during prolonged usage periods.

Figure 6. An aerial view of the 60º + 75º - 3D model inside the Immersive Virtual Environment. The violet ring represents the teleportation portal

The Accuracy Assessment process demonstrated intuitive and user-friendly characteristics. The User Interface design facilitates the visualization of key procedural aspects and offers portability, enabling users to conduct work seamlessly across various locations. This portability is particularly advantageous given the impracticality of relocating for each operation, enhancing overall efficiency. Upon calculation, statistical values are conveniently displayed within the User Interface for user reference (see Figure 7). However, there remains ample room for enhancement. Dynamic exploration of the scene and examination of Observed GCPs yielded valuable insights into the underlying causes of specific errors.

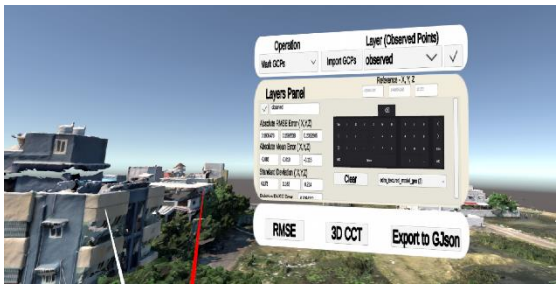

Figure 7. The User Interface of the VR Accuracy Assessment Tool displaying the calculated statistical values

The utilization of line rendering and error labelling atop the Observed spheres provided valuable insights throughout the assessment process. The rendered lines (see Figure 8) offered immediate visual feedback regarding the alignment of observed Ground Control Points (GCPs) with true spheres, enabling a rapid assessment of error direction and magnitude. This visual feedback greatly enhances decision-making processes for future planning endeavors. Additionally, the real-world visualization of surrounding features aids in comprehending the contextual factors contributing to observed errors. The incorporation of error labels (see Figure 9) facilitates the presentation of error magnitudes, functioning as an informative system for gaining insights. Furthermore, through relative accuracy calculations, a deeper understanding of the construction of 3D models is attained.

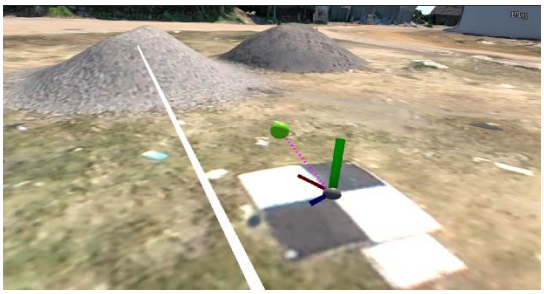

Figure 8. The error lines are drawn between the True and Observed GCPs (spheres) which helps in visualization of the errors. The red, blue and green line shows the errors along the x, y, z-axis.

Figure 9. The labels on top of the Observed points display the deviation values along the x, y, and z-axis.

In assessing the reliability of the tool, manual calculations were conducted to validate the derived relative and absolute accuracy values, yielding consistent outcomes. Nonetheless, it is imperative to investigate and cross-validate errors obtained from alternative software solutions, which constitutes a key aspect for future exploration within this study.

4.2 Influence of Camera Angles on the Absolute / Relative Accuracy and Visual Quality.

The analysis of observations from each of the four 3D models shows that the overall best performing 3D model is the 60º - 3D model in terms of z error whereas the 60º + 75º - 3D model has performed better in terms of horizontal errors. This model seems to have a good reconstruction with acceptable errors found along the z axis and the relative accuracy ($RMSE_R$) is found to be less that around 6 cm. The standard deviation (SD) values indicate that the errors within this 3D model exhibit minimal dispersion when compared to other models in the horizontal plane (x, y). However, the SD values along the z-axis are notably higher. The 75º + 90º - 3D model has drastic variations from the true values along the z axis. Errors of up to 1.2 meters were witnessed in this 3D model. On moving through the study area most of the errors were concentrated at the edges of the study area which is usually attributed with weak overlap and consequently a weak reconstruction. Also high errors were witnessed across all the four models in the northern side of the study area. This can be attributed to the impact of the adjacent water body, which likely influenced the reconstruction process. These interpretations underscore spatial variations and trends in error distribution across different models and camera angles, offering valuable insights for improvement strategies.

This contribution has been peer-reviewed. The double-blind peer-review was conducted on the basis of the full paper.
https://doi.org/10.5194/isprs-annals-X-4-2024-333-2024 | © Author(s) 2024. CC BY 4.0 License.

3D Model	60º	75°	60º + 75º	75° + 90°
$RMSE_X$	± 0.187	± 0.097	± 0.033	± 0.084
ME_X	-0.089	-0.019	-0.008	-0.019
SD_X	± 0.178	±0.096	±0.025	±0.0922
$RMSE_Y$	± 0.167	± 0.126	± 0.046	± 0.112
ME_Y	-0.05	-0.027	0.0026	-0.029
SD_Y	± 0.168	±0.118	±0.047	±0.105
$RMSE_Z$	± 0.238	± 0.366	± 0.374	± 0.824
ME_Z	-0.115	-0.0217	-0.188	-0.427
SD_Z	± 0.214	±0.3016	±0.331	±0.723
$RMSE_{Rel}$	± 0.313	± 0.187	± 0.062	± 0.158
ME_{Rel}	-0.284	-0.166	-0.527	-0.136
SD_{Rel}	±0.136	±0.088	±0.043	±0.0749

Table 3. The statistical error values in metres (m) obtained from the VR tool for each 3D model

Furthermore, a noteworthy observation is the significant increase in errors along the z axis as angles approach the nadir, although accuracy along the x and y axes improves. Notably, using an oblique angle such as the 60º - 3D model results in significantly lower errors along the z axis, yet it has the highest relative error. This phenomenon may be influenced by the predominantly horizontal placement of GCPs, where extremely acute oblique photographs exhibit relatively higher errors. It is important to validate the Relative accuracy across the vertical domain also since it provides an in depth understanding of the structural variations also.

3D Model	Structure Quality	Landscape	Fine Utilities	GCP Marker
60º	5.5	6.25	4.5	7.5
75°	4.25	4.75	4.75	6.25
60º + 75º	5.5	5.75	5.5	6.5
75°+ 90°	2.75	3.5	4	6

Table 4. Quality Score obtained by each 3D model based on the visual inspection

Following a comprehensive assessment of absolute and relative accuracies, a rigorous evaluation of multiple dimensions of the 3D models was conducted, utilizing a systematic rating system to assign quality scores on a scale of 1 to 10 based on visual inspections. Criteria such as structural integrity, vegetation coverage, delineation of fine features, utility representations, quality of Ground Control Point (GCP) markers, and terrain topography were scrutinized to gauge the overall reconstruction quality. The aggregated scores provide valuable insights into the visual fidelity of the models within the study area. Notably, the 60°-oriented 3D model demonstrated commendable scores for structural accuracy (5.5) and landscape portrayal (6.25), indicative of a visually faithful rendition. Conversely, the 75° and 75° + 90°-oriented models exhibited lower ratings in these categories, suggesting potential visual discrepancies. Fine features and utility representations garnered moderate scores across all models, while GCP marker placements consistently received high scores. Significant disparities were observed in the representation of overhead electrical lines, with their textures erroneously embedded onto roads in all 3D models. Moreover, regions containing vegetation displayed suboptimal reconstruction, particularly noticeable at closer proximity. However, at a distance, the vegetation appeared visually improved, albeit with discernible imperfections.

4.3 Pros and Cons of the VR Accuracy Assessment Tool

When visualizing 3D models on flat screens, we tend to lose the 3D perception. Typically, errors are displayed in graphs, 2D maps or 2D screens displaying the 3D model, requiring users to move or rotate the 3D model for better visualization. In immersive virtual reality (IVR), users can move around the model without disturbing its orientation while it remains static, maintaining accurate perceptions related to the direction of errors. Before performing any geospatial operations in immersive environments, such as the work demonstrated in GeaVR (Bonali et al., 2024), it is essential to know the errors in the base 3D model. In scenarios such as real-time 3D reconstruction , immersive decision-making tasks, and quantitative measurements, these tools can provide the necessary support to calculate errors before its application.

Regarding the disadvantages, the procedure demands significant computational power and can be costly. Extended use of VR can cause motion sickness; however, users generally acclimate with gradual exposure. Implementing changes such as reducing motion speed and using the teleportation tool helps in quick navigation around the 3D model. Accuracy depends on various factors, particularly human-induced errors, and initial training is necessary for using VR devices effectively. Not all assets have adequate Ground Control Point (GCP) markers, and in regions lacking GCP markers, sharp features or well-known reference points must be used for the assessment procedure. This may be challenging to identify in low-quality 3D textured meshes.

5. Conclusion

In this study, we have introduced a VR based Accuracy Assessment tool designed to validate the quality of 3D models generated by UAVs. Leveraging VR technology, our tool offers an immersive environment for visualizing spatial errors, enabling direct interactions and comprehensive assessment from data capture to mesh generation. The integration of visualization features such as color-coded Ground Control Points (GCPs), deviation markers, and data labels enhances decision-making and facilitates strategic error mitigation. This advancement represents a significant step forward in photogrammetric accuracy evaluation. A significant limitation of traditional techniques is the inability to effectively visualize errors, particularly those along the vertical axis, on a 2D screen. The loss of one dimension can impede the comprehensive understanding of errors and their dispersion. This issue is substantially mitigated in an immersive environment. Additionally, insights into occlusions during reconstruction are greatly improved in the IVR environment compared to traditional methods.

Moving forward, our future efforts will focus on refining our tool by incorporating additional parameters of the photogrammetric reconstruction process, including image geolocations, look angles, overlaps, etc. The tool can also be extended to allow users to adjust the scaling, rotation, and position of the models based on the observed errors and their dispersion. This expansion will not only deepen our understanding of the process through experimentation but also serve educational purposes, offering

enhanced visualization for teaching and learning objectives.

References

Antoniou, V., Bonali, F.L., Nomikou, P., Tibaldi, A., Melissinos, P., Mariotto, F.P., Vitello, F.R., Krokos, M., Whitworth, M., 2020. Integrating Virtual Reality and GIS Tools for Geological Mapping, Data Collection and Analysis: An Example from the Metaxa Mine, Santorini (Greece). *Applied Sciences* 10, 8317. https://doi.org/10.3390/app10238317

Barba, S., Barbarella, M., Di Benedetto, A., Fiani, M., Gujski, L., Limongiello, M., 2019. Accuracy Assessment of 3D Photogrammetric Models from an Unmanned Aerial Vehicle. *Drones* 3, 79. https://doi.org/10.3390/drones3040079

Berrett, B.E., Vernon, C.A., Beckstrand, H., Pollei, M., Markert, K., Franke, K.W., Hedengren, J.D., 2021. Large-Scale Reality Modeling of a University Campus Using Combined UAV and Terrestrial Photogrammetry for Historical Preservation and Practical Use. *Drones* 5, 136. https://doi.org/10.3390/drones5040136

Bonali, F.L., Vitello, F., Kearl, M., Tibaldi, A., Whitworth, M., Antoniou, V., Russo, E., Delage, E., Nomikou, P., Becciani, U., Van Wyk De Vries, B., Krokos, M., 2024. GeaVR: An open-source tools package for geological-structural exploration and data collection using immersive virtual reality. *Applied Computing and Geosciences* 21, 100156. https://doi.org/10.1016/j.acags.2024.100156

Chen, L., Rottensteiner, F., Heipke, C., 2021. Feature detection and description for image matching: from hand-crafted design to deep learning. *Geo-spatial Information Science* 24, 58–74. https://doi.org/10.1080/10095020.2020.1843376

Coltekin, A., Lokka, I., Zahner, M., 2016. On the usability and usefulness of 3D (geo) visualizations - A focus on virtual reality environments. *Int. Arch. Photogramm. Remote Sens. Spatial Inf. Sci.* XLI-B2, 387–392. https://doi.org/10.5194/isprsarchives-XLI-B2-387-2016

D S, D.S., N, M., S, S., D, S., R, J., G, M., 2023. Influence of quantity, quality, horizontal and vertical distribution of ground control points on the positional accuracy of UAV survey. *Applied Geomatics* 15, 897–917. https://doi.org/10.1007/s12518-023-00531-w

F. Bernardini, J. Mittleman, H. Rushmeier, C. Silva, G. Taubin, 1999. The ball-pivoting algorithm for surface reconstruction. *IEEE Transactions on Visualization and Computer Graphics* 5, 349–359. https://doi.org/10.1109/2945.817351

Furukawa, Y., Ponce, J., 2007. Accurate, Dense, and Robust Multi-View Stereopsis, in: 2007 *IEEE Conference on Computer Vision and Pattern Recognition*. pp. 1–8. https://doi.org/10.1109/CVPR.2007.383246

Gerloni, I.G., Carchiolo, V., Vitello, F.R., Sciacca, E., Becciani, U., Costa, A., Riggi, S., Bonali, F.L., Russo, E., Fallati, L., Marchese, F., Tibaldi, A., 2018. Immersive Virtual Reality for Earth Sciences. Presented at the 2018 *Federated Conference on Computer Science and Information Systems*, pp. 527–534. https://doi.org/10.15439/2018F139

Hu, D., Minner, J., 2023. UAVs and 3D City Modeling to Aid Urban Planning and Historic Preservation: A Systematic Review. *Remote Sensing* 15, 5507. https://doi.org/10.3390/rs15235507

James, M.R., Robson, S., d’Oleire-Oltmanns, S., Niethammer, U., 2017. Optimising UAV topographic surveys processed with structure-from-motion: Ground control quality, quantity and bundle adjustment. *Geomorphology* 280, 51–66. https://doi.org/10.1016/j.geomorph.2016.11.021

Kang, J., Lee, S., Yeon, S., Park, S., 2019. Improving 3D mesh quality using multi-directional UAV images. *Int. Arch. Photogramm. Remote Sens. Spatial Inf. Sci.* XLII-2/W13, 419–423. https://doi.org/10.5194/isprs-archives-XLII-2-W13-419-2019

Kazhdan, M., Bolitho, M., Hoppe, H., 2006. Poisson surface reconstruction, In: *Proceedings of the Fourth Eurographics Symposium on Geometry Processing, SGP ’06.* Eurographics Association, Goslar, DEU, pp. 61–70. doi.org/10.1145/2487228.2487237doi.org/10.1145/2487228.2487237

Kovanič, Ľ., Topitzer, B., Peťovský, P., Blišťan, P., Gergeľová, M.B., Blišťanová, M., 2023. Review of Photogrammetric and Lidar Applications of UAV. *Applied Sciences* 13, 6732. https://doi.org/10.3390/app13116732

Lague, D., Brodu, N., Leroux, J., 2013. Accurate 3D comparison of complex topography with terrestrial laser scanner: Application to the Rangitikei canyon (N-Z). *ISPRS Journal of Photogrammetry and Remote Sensing* 82, 10–26. https://doi.org/10.1016/j.isprsjprs.2013.04.009

Laksono, Aditya, 2019. Utilizing A Game Engine for Interactive 3D Topographic Data Visualization. *IJGI* 8, 361. https://doi.org/10.3390/ijgi8080361

Liu, X., Lian, X., Yang, W., Wang, F., Han, Y., Zhang, Y., 2022. Accuracy Assessment of a UAV Direct Georeferencing Method and Impact of the Configuration of Ground Control Points. *Drones* 6, 30. https://doi.org/10.3390/drones6020030

Lowe, D.G., 2004. Distinctive Image Features from Scale-Invariant Keypoints. *International Journal of Computer Vision* 60, 91–110. https://doi.org/10.1023/B:VISI.0000029664.99615.94

Luhmann, T., Chizhova, M., Gorkovchuk, D., 2020. Fusion of UAV and Terrestrial Photogrammetry with Laser Scanning for 3D Reconstruction of Historic Churches in Georgia. *Drones* 4, 53. https://doi.org/10.3390/drones4030053

Macay Moreia, J.M., Nex, F., Agugiaro, G., Remondino, F., Lim, N.J., 2013. From DSM to 3D building models: A quantitative evaluation. *The International Archives of the Photogrammetry, Remote Sensing and Spatial Information Sciences* XL-1/W1, 213–219. https://doi.org/10.5194/isprsarchives-XL-1-W1-213-2013

Manfreda, S., Dvorak, P., Mullerova, J., Herban, S., Vuono, P., Arranz Justel, J., Perks, M., 2019. Assessing the Accuracy of Digital Surface Models Derived from Optical Imagery Acquired with Unmanned Aerial Systems. *Drones* 3, 15. https://doi.org/10.3390/drones3010015

Martínez-Carricondo, P., Agüera-Vega, F., Carvajal-Ramírez, F., Mesas-Carrascosa, F.-J., García-Ferrer, A., Pérez-Porras, F.-J., 2018. Assessment of UAV-photogrammetric mapping accuracy

based on variation of ground control points. *International Journal of Applied Earth Observation and Geoinformation* 72, 1–10. https://doi.org/10.1016/j.jag.2018.05.015

Moyano, J., Nieto-Julián, J.E., Bienvenido-Huertas, D., Marín-García, D., 2020. Validation of Close-Range Photogrammetry for Architectural and Archaeological Heritage: Analysis of Point Density and 3D Mesh Geometry. *Remote Sensing* 12, 3571. https://doi.org/10.3390/rs12213571

Nex, F., Remondino, F., 2014. UAV for 3D mapping applications: a review. *Applied Geomatics* 6, 1–15. https://doi.org/10.1007/s12518-013-0120-x

Pepe, M., Alfio, V.S., Costantino, D., 2022. UAV Platforms and the SfM-MVS Approach in the 3D Surveys and Modelling: A Review in the Cultural Heritage Field. *Applied Sciences* 12, 12886. https://doi.org/10.3390/app122412886

Poux, F., Valembois, Q., Mattes, C., Kobbelt, L., Billen, R., 2020. Initial User-Centered Design of a Virtual Reality Heritage System: Applications for Digital Tourism. *Remote Sensing* 12, 2583. https://doi.org/10.3390/rs12162583

Room, M.H.M., Ahmad, A., Rosly, M.A., 2019. Assessment of different unmanned aerial vehicle system for production of photogrammetry products. *Int. Arch. Photogramm. Remote Sens. Spatial Inf. Sci.* XLII-4/W16, 549–554. https://doi.org/10.5194/isprs-archives-XLII-4-W16-549-2019

Rossi, P., Mancini, F., Dubbini, M., Mazzone, F., Capra, A., 2017. Combining nadir and oblique UAV imagery to reconstruct quarry topography: methodology and feasibility analysis. *European Journal of Remote Sensing* 50, 211–221. https://doi.org/10.1080/22797254.2017.1313097

Sarkar, D., Sinha, R., Bookhagen, B., 2023. Towards a Guideline for UAV-Based Data Acquisition for Geomorphic Applications. *Remote Sensing* 15, 3692. https://doi.org/10.3390/rs15143692

Seitz, S.M., Curless, B., Diebel, J., Scharstein, D., Szeliski, R., 2006. A Comparison and Evaluation of Multi-View Stereo Reconstruction Algorithms, in: 2006 *IEEE Computer Society Conference on Computer Vision and Pattern Recognition (CVPR'06)*. pp. 519–528. https://doi.org/10.1109/CVPR.2006.19

Singh, P.S., Sharma, M., Saikhom, V., Chutia, D., Gupta, C., Chouhan, A., Raju, P.L.N., 2018. Towards Generation of Effective 3D Surface Models from UAV Imagery Using Open Source Tools. *Current Science* 114, 314. https://doi.org/10.18520/cs/v114/i02/314-321

Snavely, N., Seitz, S.M., Szeliski, R., 2008. Modeling the World from Internet Photo Collections. *International Journal of Computer Vision* 80, 189–210. https://doi.org/10.1007/s11263-007-0107-3

Stott, E., Williams, R.D., Hoey, T.B., 2020. Ground Control Point Distribution for Accurate Kilometre-Scale Topographic Mapping Using an RTK-GNSS Unmanned Aerial Vehicle and SfM Photogrammetry. *Drones* 4, 55. https://doi.org/10.3390/drones4030055

Szczepańska, A., Kaźmierczak, R., Myszkowska, M., 2021. Virtual Reality as a Tool for Public Consultations in Spatial Planning and Management. *Energies* 14, 6046. https://doi.org/10.3390/en14196046

Tibaldi, A., Bonali, F.L., Vitello, F., Delage, E., Nomikou, P., Antoniou, V., Becciani, U., De Vries, B.V.W., Krokos, M., Whitworth, M., 2020. Real world–based immersive Virtual Reality for research, teaching and communication in volcanology. *Bull Volcanol* 82, 38. https://doi.org/10.1007/s00445-020-01376-6

Westoby, M.J., Brasington, J., Glasser, N.F., Hambrey, M.J., Reynolds, J.M., 2012. ‘Structure-from-Motion’ photogrammetry: A low-cost, effective tool for geoscience applications. *Geomorphology* 179, 300–314. https://doi.org/10.1016/j.geomorph.2012.08.021